



Cite this: RSC Adv., 2015, 5, 9703

 Received 28th November 2014
 Accepted 6th January 2015

DOI: 10.1039/c4ra15437a

www.rsc.org/advances

We report the use of fumed silica (hydrophilic colloidal silica particles) to generate triglyceride solvent-based soft matter systems (organogels and bigels). Interestingly, the bigels showed a better gel strength compared to organogels while showing a comparatively weaker thixotropic recovery. Electron microscopy and energy dispersive X-ray spectroscopy were used to understand the microstructure of these new thixotropic molecular gel systems with respect to the fractal-like aggregation of silica particles as well as the percolating network of organic-aqueous phases.

In the last few years, the research on structuring of triglyceride solvents (vegetable oils) has received considerable interest from both academic as well as industrial researchers. The possibility of transforming liquid oils into soft, viscoelastic gels (organogels) opens up a number of opportunities for applications such as the development of *trans* and saturated fat-free food products,^{1–4} transdermal drug delivery systems,⁵ bio-based lubricants⁶ and analysis and purification-related systems.⁷ Since the applications of organogels range from non-bio to bio-related fields, the choice of structurants determines the suitability of using organogels in a range of unrelated fields. Accordingly, a lot of effort has been focused on identifying newer structurants either by synthesizing new materials^{8,9} or by studying the oil gelling properties of known raw materials such as waxes, cellulose derivatives, proteins, fatty acids, cyclodextrins, phytosterols *etc.*^{10–17}

Colloidal silicon dioxide (fumed silica) is among the most researched inorganic particles that have relevant industrial applications in fields including pharmaceuticals, cosmetics, foods, ceramics, electronics *etc.*^{18,19} From colloidal science point of view, the microstructure of fumed silica (Fig. 1) is quite

^aVandemoortele 'Lipid Science & Technology', Lab. of Food Tech. & Engg., Faculty of Bioscience Engg., Ghent University, Coupure Links 653, 9000 Gent, Belgium. E-mail: Patel.Ashok@Ugent.be

^bVandemoortele R&D Izegem, Prins Albertlaan 79, 8870 Izegem, Belgium

† Electronic supplementary information (ESI) available. See DOI: 10.1039/c4ra15437a

interesting and can be viewed at three different length scales, comprising of primary particles (size range = 5–50 nm) fused into stable fractal aggregates (size range = 100–500 nm) which further grow into micron-size agglomerates stabilized by hydrogen bonding and electrostatic interactions.^{20,21} This unique branched structure with large specific surface area and surface hydrophilicity is the reason for the extensive use of fumed silica as a thickening and gelling agent for aqueous, ionic and organic solvents.^{22–26} Colloidal silicon particles are also known to be surface active and thus, have been explored for the fabrication of particle-stabilized emulsions and foams.^{27–30} In addition to these excellent properties, fumed silica (along with other types of synthetic amorphous silica) has a GRAS (Generally Recognized As Safe) status and is approved for direct and indirect food uses (E 551).

In this paper, we report for the first time, the use of fumed silica as a structurant to gel a triglyceride solvent (vegetable oil) and further use this as an organic phase in combination with a

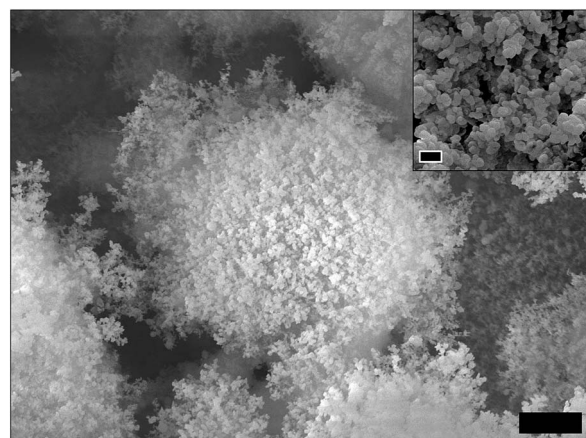


Fig. 1 Scanning electron microscopy image of fumed silica showing the micro-scale agglomerates (scale bar = 5 μ m). Inset: the magnified image showing the underlying sub-micron structures (scale bar = 500 nm).



'weak' water gel to create 'aqueous-organic' bigels with a complex microstructure that results in interesting rheological properties. Oscillatory and flow measurements were carried out to gain important insights into the structure–property relationship of organogels and bigels. Electron microscopy in combination with energy dispersive X-ray spectroscopy (EDS) was used to visualize the microstructure of systems as well as to study the distribution of silica particles in the bigel sample.

Hydrophilic fumed silica (A150) was used to structure sunflower oil at 4 different concentrations (2.5, 5, 10 and 15 wt%) by dispersing the weighed amount of A150 fluffy powder in liquid sunflower oil at room temperature under high shear (at 11 000 rpm). As seen from Fig. 2a and d, at lower concentrations (2.5 and 5 wt%), fumed silica formed viscous sols displaying almost negligible yield stresses (0.3 and 2.4 Pa respectively) and a weak pseudoplastic flow behaviour (flow index = 0.89 and 0.83 respectively). On the other hand, the relatively higher concentrations (10 and 15 wt%) produced viscoelastic gels that resisted flow even when subjected to stress values as high as 400 Pa. The oil viscosifying property of fumed silica is well-known (attributed to a 3D network formation in liquid oil) and accordingly, the fumed silica is often used for rheology control of mineral and vegetable oils.³¹ In our study, we found that at a higher concentration of fumed silica (≥ 10 wt%), a gel formation is possible if the fumed silica is dispersed uniformly under high shear. The higher concentration should result in a higher particle–particle interactions leading to a stronger network formation that is able to resist small deformations. More details on the network formation is discussed later with the help of microscopy images. The results from the oscillatory measurements (amplitude sweeps) are shown in Fig. 2e. As seen from the graph, the complex modulus, G^* (a measure of the total resistance of the material to the applied shear) and the linear viscoelastic region (region constituting the

linear response of input stress and output strain) were significantly higher and broader respectively for samples prepared at higher concentrations (10 and 15 wt%) as compared to the samples made at concentrations of 2.5 and 5 wt%, thus, indicating the relative strength of the microstructures of these samples. The values for oscillatory yield stress (where elastic modulus, G' equals viscous modulus, G'' , indicated on graph by dashed red line corresponding to phase angle of 45 degrees) obtained for the 4 samples were as follows: 2.5 wt% = 0.71 Pa; 5 wt% = 4.98 Pa; 10 wt% = 95.6 Pa and 15 wt% = 4775 Pa. Based on the above results, it is clear that among the studied concentrations, 15 wt% of A150 forms a viscoelastic gel with high gel strength that shows strongest resistance to the permanent deformation (yielding) under applied stress conditions. Hence, the gel prepared at 15 wt% A150 (Fig. 2b) was selected for all further studies. Further, a weak water gel structured using a combination of polysaccharides (1 wt% of locust bean gum: carrageenan, LBG : Car at 1 : 1 ratio) was mixed with 15 wt% A150 organogel in different proportions to obtain 'aqueous-organic' bigels. A representative picture of a bigel prepared at organogel : water gel (O : W) ratio of 9 : 1 is shown in Fig. 2c.

Bigels are bicontinuous systems which are a relatively unexplored class of soft matter systems.^{32–34} Due to their complex microstructure, bigels display interesting rheological properties.^{32,35} The rheological properties of bigels prepared at different O : W ratios (9 : 1, 8 : 2, 7 : 3 and 6 : 4) were studied using oscillatory amplitude sweeps. The data from amplitude stress sweeps done on water gel, organogel and bigels is shown in Fig. 3. A synergistic combination of LBG : Car usually results in a water gel which is weakly structured as reported by us earlier.³⁶ The lower values of elastic and viscous moduli confirms the 'weak' structure of water gel as compared to organogel which showed a strong gel behaviour with value of $G' \sim 10^4$ Pa that was higher than G'' by more than a decade in LVR (Fig. 3a). Interestingly, all the bigel samples showed higher gel strengths than the organogel as indicated by G' values much higher than 10^4 Pa along with a relatively bigger difference between G' and G'' as well as higher values of oscillatory yield stresses ($> 10^3$ Pa) (Fig. 3b). Di Michele L. *et al.* recently used numerical model to prove that a bigel is capable of bearing significantly higher stress compared to a one-component gel.³²

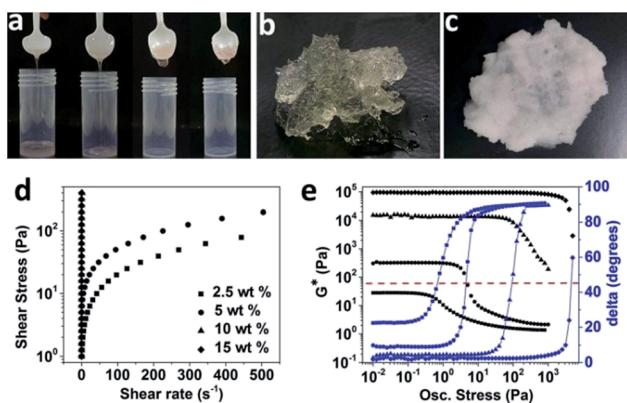


Fig. 2 (a) Photograph showing the flow behaviour of sunflower oil dispersions containing from left to right 2.5, 5, 10 and 15 wt% of A150; (b) & (c) photographs of an organogel (sunflower oil with 15 wt% A150) and a bigel (O : W ratio of 9 : 1) respectively; (d) & (e) comparative curves from stress ramp and amplitude sweeps for sunflower oil dispersions containing 2.5, 5, 10 and 15 wt% of A150. Note: the flow curves for 2.5 and 5 wt% samples were fitted to Hershel–Bulkley model (see ESI† for more details) and also note that the figure legends in Fig. 2d applies to Fig. 2e as well.

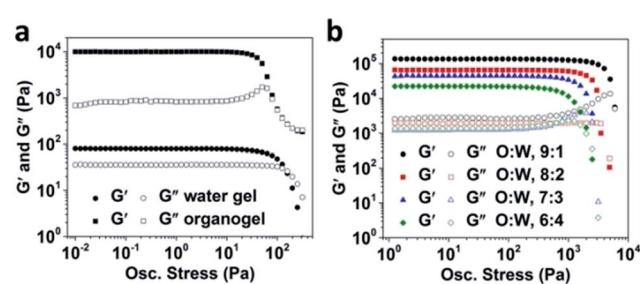


Fig. 3 (a) Amplitude stress sweeps (elastic and viscous moduli, G' and G'' versus oscillatory stress) of water gel (prepared using 1 wt% LBG : Car at a ratio of 1 : 1) and organogel (at 15 wt% A150); (b) amplitude stress sweeps for bigels prepared at different O : W ratios.



The shape of curves indicate that the rheological response of bigels is highly dominated by the organogel component at all the studied O : W ratios. However, since, all the bigels showed a higher gel strength compared to organogel, we speculate that the formation of semi-continuous interpenetrating phases of oil and water in bigels contributes to the overall rheology of the samples. Further, a clear influence of increasing the water gel proportion on the lowering of gel strength was also observed as expected. We also observed that the bigels prepared at O : W ratios of 5 : 5 to 1 : 9 did not gel but behaved like viscous sols and hence were excluded from the study.

The organogels prepared using fumed silica were transparent in appearance (Fig. 4a) suggesting that the structuring units (silica particles) in the gels are considerably smaller than the wavelength of visible light (wavelength range: 400–750 nm). The scattering of light (Faraday–Tyndall effect)³⁷ illustrated in

Fig. 4b further confirms the colloidal size range of silica particles and strongly implies a possible de-agglomeration of fumed silica particles.

The microstructure of organogel and bigel was studied using a combination of techniques including cryo-SEM, confocal microscopy and energy dispersive X-ray spectroscopy (EDS). For imaging of organogel, the sample preparation was carried out by first removing the surface oil (using butanol as a solvent), a technique commonly referred to as de-oiling.^{38,39} The cryo-SEM image of de-oiled organogel sample shown in Fig. 4c, indicates the presence of a fractal-like network of colloidal silicon particles which is responsible for trapping the liquid oil in the gel structure. In fact, the role played by the fractal aggregation of fumed silica in gelation of a range of solvent has been extensively investigated and is believed to be caused due to the hydrogen bonding mediated by the silanol groups (Si–OH) present on the particle surface.^{23,24,40} The fractal aggregate formation is much stronger in non-polar solvents that are not capable of forming hydrogen bonding hence, promoting more particle–particle interactions.^{40,41} In contrast, hydrophobic fumed silica (where the silanol surface groups are modified with hydrophobic moieties) tend to show a weak gelling behaviour because of the decrease in the hydrogen bonding sites.²⁴ To verify this, the gelation of oil by hydrophobic fumed silica (A972) was studied through rheological measurements and compared to A150 (Fig. 5a). As expected, the A972 formed a weaker gel compared to A150 as confirmed from the lower values of G' and G'' which showed a strong frequency dependence and a prominent crossover point at a higher frequency. In contrast, the A150 organogel showed a strong gel characteristic (mainly elastic dominant) with only a slight dependence on the frequency with $\tan \delta (G''/G')$ values much lower than unity throughout the studied frequency.

The bigel was subjected to a range of visualization techniques to understand the distribution of organic and aqueous phases. Confocal microscopy image shown in Fig. 4d clearly displays the discontinuous distribution of water phase (unstained) in the stained oil phase (false green colour). The bicontinuous microstructure of the bigel can be seen from the 3D volume views constructed from stacks of confocal microscopy images of bigel samples prepared at O : W ratios of 9 : 1 and 6 : 4 (Fig. 4e and f). The distribution pattern of oil and water phases is also visible in the cryo-SEM image taken on a freeze fractured sample (Fig. 4g). The removal of water through sublimation left a porous mesh of polymer matrix interspersed between the discontinuous oil solid phase. This focused area of the sample was also subjected EDS analysis and the elemental map of Si created based on the spectral analysis is shown in Fig. 4h and S1.† Interestingly, the elemental map indicates that the silica particles preferred to partition from oil phase into the water phase owing to their hydrophilic nature. In addition, due to the presence of multiple binding sites on the polymer molecules, a surface adsorption-based interaction of polymer chains with silica particles in the water phase is also possible.^{42,43}

The rheological properties of bigels were compared through flow and oscillatory measurements in order to understand the

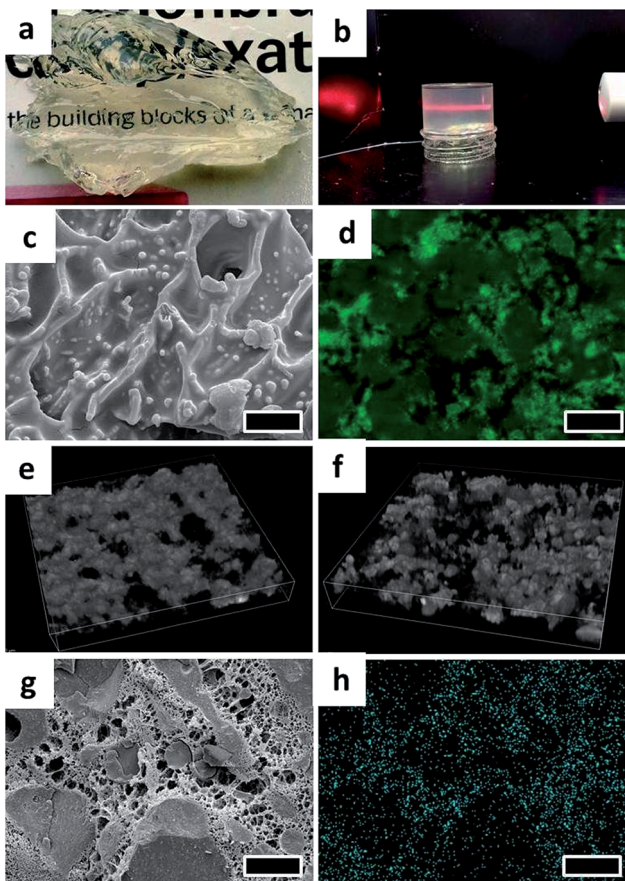


Fig. 4 (a) Photograph of transparent organogel prepared at 15 wt%; (b) Faraday–Tyndall effect observed when a laser beam is passed through the organogel sample; (c) cryo SEM image of 15 wt% A150 organogel where surface oil was removed using butanol (scale bar = 1 μ m); (d) bigel prepared at O : W ratio of 8 : 2 imaged under confocal microscope (scale bar = 25 μ m); (e) & (f) 3D volume views of bigel samples prepared at O : W ratios of 9 : 1 and 6 : 4 respectively (dimensions: x and y = 104.67 μ m and z = 18 μ m); (g) & (h) cryo-SEM image of bigel prepared at O : W ratio of 6 : 4 imaged after sublimation of water and the corresponding elemental map showing the distribution of silicon (shown in blue-green) in the bigel sample as recorded using EDS (scale bar = 10 μ m).

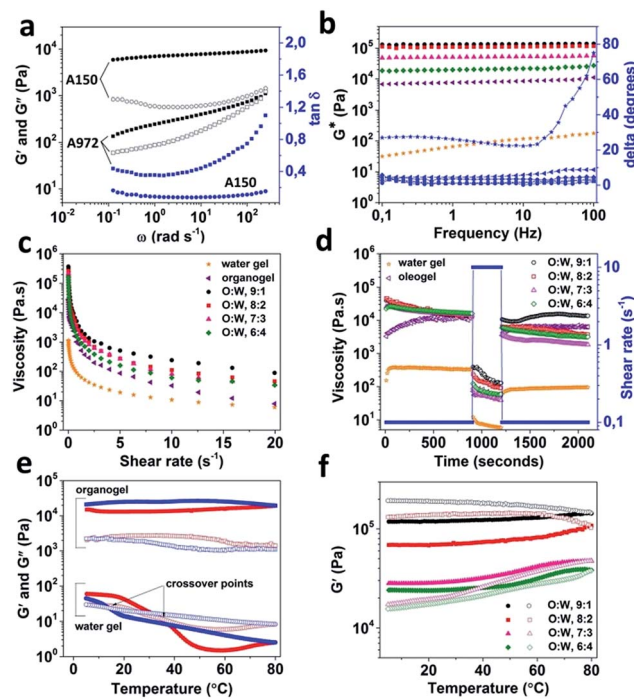


Fig. 5 (a) Comparative plots from frequency sweeps of organogels prepared using 15 wt% of hydrophilic (A 150) and hydrophobic (A 972) silica particles; (b) & (c) curves from frequency sweeps and flow measurements respectively for water gel, organogel and bigels prepared at different O : W ratios, the figure legends in (c) applies to (b) as well; (d) curves from 3 interval thixotropy test done on water gel, organogel and bigels prepared at different O : W ratios; (e) G' and G'' measured as a function of temperature for water gel and organogel subjected to heating (red symbols) and cooling (blue symbols) steps, the filled and open symbols represent G' and G'' respectively; (f) G' measured as a function of temperature for bigels prepared at different O : W ratios, filled and open symbols represent heating and cooling steps respectively.

influence of organic and aqueous phase proportions on the overall rheology of the bigels. The frequency and flow curves for water gel, organogel and bigels are shown in Fig. 5b and c respectively. As seen from Fig. 5b, the weak gel characteristics of water gel is confirmed from low values of complex modulus (G^*) that showed frequency dependence. Moreover, a gel-sol transformation (phase angle or delta degrees crossing 45°) was also observed at higher frequency values. The organogel on the other hand, showed a strong gel behaviour with high and constant values of G^* throughout the entire frequency range and phase angle values below 10°. Interestingly, the gel strength of bigels (at all O : W ratios) was significantly higher than organogel, suggesting a synergistic enhancement of the rheology due to the mixing of structured organic and aqueous phases. The synergistic effect on rheology of bigels could be explained from the inter penetrating network of organic and aqueous phases. It has recently been understood that similar to the colloidal gel formation seen in case of short-ranged attractive colloids (SRAC), arrested de-mixing of binary colloidal mixtures also results in ramified space-spanning structures (bigels) due to an interplay of phase separation and arrest.^{34,44} Moreover, it was

recently confirmed in the work of Di Michele L. *et al.*³² that the bigels formed due to the arrested de-mixing of two component systems have better rheological properties compared to one component gels. As proved using cluster analysis, the enhancement in the rheological properties of two component gel is due to the rearrangement of particles under deformation into multiple smaller clusters instead of a single compact cluster seen in one component gels.³² The bigels did show a decrease in the gel strength with increasing proportion of water phase which probably is due to the increased partitioning of silica particles in the water phase as discussed previously. The flow behaviour shown in Fig. 5c suggest a pseudoplastic behaviour for both the water gel and the organogel. However, the viscosity of organogel at rest was significantly higher compared to that of water gel. The bigels also showed pseudoplastic flow properties and the viscosity values at rest showed a decrease with the increase in the water gel proportion. In addition, the effect of time and shear history on the viscosity of bigels was studied using a 3 interval thixotropy test (3-ITT) to understand the structure recovery properties. As seen from Fig. 5d, water gel and organogel showed completely different behaviour as a function of time at alternating low and high shear rates (0.1 and 10 s⁻¹ respectively). While, water gel showed no apparent change in the viscosity values over time at a low shear rate (0.1 s⁻¹) in the first interval, the viscosity of organogel increased with time. This behaviour of organogel is indicative of rheopexy or negative thixotropy and is attributed to the clustering of aggregates of silica particles as reported in the literature.^{43,45-48} Unlike water gel, organogel also showed a complete structure recovery when shear rate was changed back to lower value in the third interval. Interestingly, the bigel samples (prepared at all O : W ratios) showed thixotropic behaviour (decrease in viscosity values with time at constant shear rate) in the first interval while showing only a partial structure recovery in the third interval. For more details, the values for viscosity (in interval 1 and 3) and % recovery can be referred from Table S1 provided as ESI.†

In addition, the influence of temperature on the micro-structure of bigels was also studied and compared to the temperature behaviour of water gel and organogel (Fig. 5e and f). As seen from Fig. 5e, the water gel showed a clear gel-to-sol transformation on heating and a reversible gelation on cooling (confirmed from two distinct crossover points) with a well-defined hysteresis (temperature difference between melting and re-gelation of the sample). On the other hand, organogel showed a slight increase in the gel strength (indicated by an increase in the G' value) when subjected to heating which did not return to its initial value on cooling. Such temperature induced irreversible restructuring and increase in the network strength of hydrophilic silica particles in apolar solvents has been explained using fractal gel model in detailed work of Wu and co-workers.²¹ They observed an increase in the fractal dimension at high temperatures indicating more compact packing and thus a stronger H-bonding due to the closeness of packed particles.²¹ Bigels, on the other hand, displayed a much higher increase in the gel strength during the heating step (Fig. 5f), a plausible explanation for this behaviour could be



related to the possible interactions of silica particles with the polymer chains in the aqueous phase. Such interactions of silica particles with hydrophilic polymers in aqueous solvent has been reported for silica particles in aqueous hydroxyl propyl methylcellulose solutions.^{49,50} When comparing the rheological response during the cooling step, two different kind of behaviour was observed. In case of samples with relatively higher proportion of organogel phase (O : W = 9 : 1 and 8 : 2), the final values of the elastic moduli after the cooling step was higher than the initial values. Whereas, for the other two samples, the final values were much lower than the initial values. The bigels (as seen from Fig. S2†) display a different percolating structure based on the organic-aqueous phase ratios used in their preparation. As the proportion of water phase is increased, the microstructure shows a defined change from a one component percolation network to a double percolation or two component percolation network³⁴ which could further result in the partition of a greater proportion of silica particles in the aqueous phase interfering with the restructuring of silica particles and the consequent strengthening of particle network on cooling.

In conclusion, the oil structuring properties of fumed silica was exploited for the very first time to prepare triglyceride solvent-based organogel as well as a relatively new class of soft matter systems called bigels. The dispersion of fumed silica in a triglyceride solvent at high concentration (10 wt% and above) results in the formation of a gel where the liquid solvent is physically trapped in a 3D network based on the fractal aggregation of silica particles. The addition of water gel to structured oil leads to the formation of bigels where both the organic and the aqueous phases are distributed as percolating network. The rheological properties of bigels were completely different from either of the individual component gels. While, the bigels showed a comparatively higher gel strength, the structure recovery behaviour was much weaker than the organogel. Moreover, the rheological properties was significantly influenced by the proportion of organic and aqueous phases used and thus, this opens up new possibilities of tuning the bigel properties.

Acknowledgements

This research is supported by the Marie Curie Career Integration Grant (Project: SAT-FAT-FREE) within the 7th European Community Framework Programme. Hercules foundation is acknowledged for its financial support in the acquisition of the scanning electron microscope JEOL JSM-7100F equipped with cryo-transfer system Quorum PP3000T and Oxford Instruments Aztec EDS (grant number AUGE-09-029).

Notes and references

- 1 N. E. Hughes, A. G. Marangoni, A. J. Wright, M. A. Rogers and J. W. E. Rush, *Trends Food Sci. Technol.*, 2009, **20**, 470–480.
- 2 A. R. Patel, P. S. Rajarethinem, A. Gredowska, O. Turhan, A. Lesaffer, W. H. De Vos, D. Van de Walle and K. Dewettinck, *Food Funct.*, 2014, **5**, 645–652.
- 3 A. R. Patel, N. Cludts, M. D. B. Sintang, A. Lesaffer and K. Dewettinck, *Food Funct.*, 2014, **5**, 2833–2841.
- 4 N. E. Hughes, A. G. Marangoni, A. J. Wright, M. A. Rogers and J. W. E. Rush, *Trends Food Sci. Technol.*, 2009, **20**, 470–480.
- 5 A. Vintiloiu and J.-C. Leroux, *J. Controlled Release*, 2008, **125**, 179–192.
- 6 T. A. Stortz and A. G. Marangoni, *Green Chem.*, 2014, **16**, 3064–3070.
- 7 W. L. Hinze, I. Uemasu, F. Dai and J. M. Braun, *Curr. Opin. Colloid Interface Sci.*, 1996, **1**, 502–513.
- 8 J. H. van Esch and B. L. Feringa, *Angew. Chem., Int. Ed.*, 2000, **39**, 2263–2266.
- 9 P. Terech and R. G. Weiss, *Chem. Rev.*, 1997, **97**, 3133–3160.
- 10 A. R. Patel, D. Schatteman, W. H. D. Vos and K. Dewettinck, *RSC Adv.*, 2013, **3**, 5324–5327.
- 11 M. Pernetti, K. F. van Malssen, E. Flöter and A. Bot, *Curr. Opin. Colloid Interface Sci.*, 2007, **12**, 221–231.
- 12 A. G. Marangoni and N. Garti, *Edible oleogels: Structure and health implications*, AOCS Press, Urbana, Illinois, 2011.
- 13 A. R. Patel, D. Schatteman, A. Lesaffer and K. Dewettinck, *RSC Adv.*, 2013, **3**, 22900–22903.
- 14 A. R. Patel, N. Cludts, M. D. Bin Sintang, B. Lewille, A. Lesaffer and K. Dewettinck, *ChemPhysChem*, 2014, **15**, 3435–3439.
- 15 A. R. Patel, P. S. Rajarethinem, N. Cludts, B. Lewille, W. H. De Vos, A. Lesaffer and K. Dewettinck, *Langmuir*, 2014, DOI: 10.1021/la502829u.
- 16 T. Kida, Y. Marui, K. Miyawaki, E. Kato and M. Akashi, *Chem. Commun.*, 2009, 3889–3891.
- 17 H. Sawalha, R. den Adel, P. Venema, A. Bot, E. Flöter and E. van der Linden, *J. Agric. Food Chem.*, 2012, **60**, 3462–3470.
- 18 O. W. Flörke, H. A. Graetsch, F. Brunk, L. Benda, S. Paschen, H. E. Bergna, W. O. Roberts, W. A. Welsh, C. Libanati, M. Ettlinger, D. Kerner, M. Maier, W. Meon, R. Schmoll, H. Gies and D. Schiffmann, in *Ullmann's Encyclopedia of Industrial Chemistry*, Wiley-VCH Verlag GmbH & Co. KGaA, 2000.
- 19 H. Ferch, *Prog. Org. Coat.*, 1982, **10**, 91–118.
- 20 V. M. Gun'ko, I. F. Mironyuk, V. I. Zarko, V. V. Turov, E. F. Voronin, E. M. Pakhlov, E. V. Goncharuk, R. Leboda, J. Skubiszewska-Zięba, W. Janusz, S. Chibowski, Y. N. Levchuk and A. V. Klyueva, *J. Colloid Interface Sci.*, 2001, **242**, 90–103.
- 21 X.-J. Wu, Y. Wang, W. Yang, B.-H. Xie, M.-B. Yang and W. Dan, *Soft Matter*, 2012, **8**, 10457–10463.
- 22 V. M. Gun'ko, I. F. Mironyuk, V. I. Zarko, E. F. Voronin, V. V. Turov, E. M. Pakhlov, E. V. Goncharuk, Y. M. Nychiporuk, N. N. Vlasova, P. P. Gorbik, O. A. Mishchuk, A. A. Chuiko, T. V. Kulik, B. B. Palyanytsya, S. V. Pakhovichishin, J. Skubiszewska-Zięba, W. Janusz, A. V. Turov and R. Leboda, *J. Colloid Interface Sci.*, 2005, **289**, 427–445.
- 23 W. E. Smith and C. F. Zukoski, *J. Colloid Interface Sci.*, 2006, **304**, 359–369.
- 24 J. Nordstrom, A. Matic, J. Sun, M. Forsyth and D. R. MacFarlane, *Soft Matter*, 2010, **6**, 2293–2299.



25 S. R. Raghavan, H. J. Walls and S. A. Khan, *Langmuir*, 2000, **16**, 7920–7930.

26 K. Ueno, K. Hata, T. Katakabe, M. Kondoh and M. Watanabe, *J. Phys. Chem. B*, 2008, **112**, 9013–9019.

27 B. P. Binks, *Curr. Opin. Colloid Interface Sci.*, 2002, **7**, 21–41.

28 B. P. Binks and T. S. Horozov, *Angew. Chem.*, 2005, **117**, 3788–3791.

29 A. Perino, C. Noïk and C. Dalmazzone, *Energy Fuels*, 2013, **27**, 2399–2412.

30 A. Stocco, E. Rio, B. P. Binks and D. Langevin, *Soft Matter*, 2011, **7**, 1260–1267.

31 Technical Information TI 1279, Successful use of AEROSIL® fumed silica in liquid systems, Evonik Industries.

32 L. Di Michele, D. Fiocco, F. Varrato, S. Sastry, E. Eiser and G. Foffi, *Soft Matter*, 2014, **10**, 3633–3648.

33 V. K. Singh, A. Anis, I. Banerjee, K. Pramanik, M. K. Bhattacharya and K. Pal, *Mater. Sci. Eng., C*, 2014, **44**, 151–158.

34 F. Varrato, L. Di Michele, M. Belushkin, N. Dorsaz, S. H. Nathan, E. Eiser and G. Foffi, *Proc. Natl. Acad. Sci. U. S. A.*, 2012, **109**, 19155–19160.

35 V. K. Singh, I. Banerjee, T. Agarwal, K. Pramanik, M. K. Bhattacharya and K. Pal, *Colloids Surf., B*, 2014, **123**, 582–592.

36 A. R. Patel, Y. Rodriguez, A. Lesaffer and K. Dewettinck, *RSC Adv.*, 2014, **4**, 18136–18140.

37 E. O. Kraemer and S. T. Dexter, *J. Phys. Chem.*, 1926, **31**, 764–782.

38 M. Rogers, A. Smith, A. Wright and A. Marangoni, *J. Am. Oil Chem. Soc.*, 2007, **84**, 899–906.

39 A. K. Zetzl, A. J. Gravelle, M. Kurylowicz, J. Dutcher, S. Barbut and A. G. Marangoni, *Food Struct.*, 2014, **2**, 27–40.

40 W. E. Smith and C. F. Zukoski, *J. Colloid Interface Sci.*, 2006, **304**, 348–358.

41 S. A. Khan and N. J. Zoeller, *J. Rheol.*, 1993, **37**, 1225–1235.

42 S. K. Parida, S. Dash, S. Patel and B. K. Mishra, *Adv. Colloid Interface Sci.*, 2006, **121**, 77–110.

43 M. Kawaguchi, *Adv. Colloid Interface Sci.*, 1994, **53**, 103–127.

44 P. J. Lu, E. Zaccarelli, F. Ciulla, A. B. Schofield, F. Sciortino and D. A. Weitz, *Nature*, 2008, **453**, 499–503.

45 Y. Nakai, Y. Ryo and M. Kawaguchi, *J. Chem. Soc., Faraday Trans.*, 1993, **89**, 2467–2472.

46 B. Jaúregui-Beloqui, J. C. Fernández-García, A. César Orgilés-Barceló, M. Mar Mahiques-Bujanda and J. M. Martín-Martínez, *Int. J. Adhes. Adhes.*, 1999, **19**, 321–328.

47 J.-H. So, W.-K. Oh and S.-M. Yang, *Korean J. Chem. Eng.*, 2004, **21**, 921–928.

48 J.-H. So, S.-M. Yang, C. Kim and J. C. Hyun, *Colloids Surf., A*, 2001, **190**, 89–98.

49 M. Kawaguchi, Y. Kimura, T. Tanahashi, J. Takeoka, J.-i. Suzuki, T. Kato and S. Funahashi, *Langmuir*, 1995, **11**, 563–567.

50 M. Kawaguchi, R. Naka, M. Imai and T. Kato, *Langmuir*, 1995, **11**, 4323–4327.

